Transcranial Magnetic Resonance Imaging–Guided Focused Ultrasound Surgery of Brain Tumors: Initial Findings in 3 Patients

Nathan McDannold, PhD

Department of Radiology,
Brigham and Women's Hospital,
Harvard Medical School,
Boston, Massachusetts

Greg T. Clement, PhD

Department of Radiology,
Brigham and Women's Hospital,
Harvard Medical School,
Boston, Massachusetts

Peter Black, MD

Departments of Radiology and Neurosurgery,
Brigham and Women's Hospital,
Boston, Massachusetts,

Ferenc Jolesz, MD

Department of Radiology,
Brigham and Women's Hospital,
Harvard Medical School,
Boston, Massachusetts

Kullervo Hynynen, PhD

Department of Radiology,
Brigham and Women's Hospital,
Boston, Massachusetts, and
Department of Medical Biophysics,
University of Toronto and
Sunnybrook Health Sciences Centre,
Toronto, Canada

Reprint requests:
Nathan McDannold, PhD,
Department of Radiology,
Brigham and Women's Hospital,
221 Longwood Avenue (LMRC 521),
Boston, MA 02115.
E-mail: njm@bwh.harvard.edu

Received, December 26, 2008.
Accepted, May 28, 2009.

OBJECTIVE: This work evaluated the clinical feasibility of transcranial magnetic resonance imaging–guided focused ultrasound surgery.

METHODS: Transcranial magnetic resonance imaging–guided focused ultrasound surgery offers a potential noninvasive alternative to surgical resection. The method combines a hemispherical phased-array transducer and patient-specific treatment planning based on acoustic models with feedback control based on magnetic resonance temperature imaging to overcome the effects of the cranium and allow for controlled and precise thermal ablation in the brain. In initial trials in 3 glioblastoma patients, multiple focused ultrasound exposures were applied up to the maximum acoustic power available. Offline analysis of the magnetic resonance temperature images evaluated the temperature changes at the focus and brain surface.

RESULTS: We found that it was possible to focus an ultrasound beam transcranially into the brain and to visualize the heating with magnetic resonance temperature imaging. Although we were limited by the device power available at the time and thus seemed to not achieve thermal coagulation, extrapolation of the temperature measurements at the focus and on the brain surface suggests that thermal ablation will be possible with this device without overheating the brain surface, with some possible limitation on the treatment envelope.

CONCLUSION: Although significant hurdles remain, these findings are a major step forward in producing a completely noninvasive alternative to surgical resection for brain disorders.

KEY WORDS: Ablation techniques, Brain, Magnetic resonance imaging, Tumor, Ultrasonic therapy

Neurosurgery 66:323-332, 2010 DOI: 10.1227/01.NEU.0000360379.95800.2F www.neurosurgery-online.com

Despite progress made in many cancer treatments, brain tumors remain an extraordinary challenge. Because of the inherent risks with associated surgical resection and radiotherapy, combined with the aggressiveness of many central nervous system tumors and the difficulty in delivering anticancer drugs to the brain, the prognosis for patients with many types of brain tumors remains grim. New and less invasive alternatives to existing procedures are desperately needed.

Thermal ablation has been pursued as an alternative to surgery for tumor therapy in several targets, including the brain.[1-3] It can be used to destroy tumors with few or no effects to the surrounding tissue, producing immediate and localized thermal coagulation. It can be used along with, potentially synergistically with, radiotherapy or chemotherapy. Thermal ablation, which does not use ionizing radiation, can also be reapplied in the case of recurrence.

ABBREVIATIONS: CT, computed tomography; **MRI**, magnetic resonance imaging; **MRTI**, magnetic resonance temperature imaging; **ROI**, region of interest; **TcMRgFUS**, transcranial magnetic resonance imaging–guided focused ultrasound surgery

A completely noninvasive approach to thermal ablation that has been tested for more than 60 years has been focused ultrasound. An ultrasound beam can be precisely focused deep into soft tissue. High intensities, resulting in localized heating caused by absorption of the acoustic wave, can be achieved in the focal zone without damaging the surrounding tissues. Since the first tests, focused ultrasound has been investigated for the treatment of brain disorders.[4] Pioneering work by Fry et al,[5,6] and others[7-11] showed the huge potential of this technology in animal trials, and

promising clinical treatments of neurological disorders were performed.[12,13] Despite the early promise, the use of focused ultrasound, particularly in the brain, has not reached widespread use. The challenge has been because of 2 main obstacles: a lack of control of the procedure and the difficulty in applying ultrasound through the cranium.

Improvements in medical imaging have led to a resurgence of interest in focused ultrasound in recent decades. Ultrasound imaging, which allows some ability to target the beam, and, more significantly, magnetic resonance imaging (MRI), which allows exquisite targeting and feedback control of the procedure with quantitative temperature imaging,[14] have led to several focused ultrasound systems designed for a wide range of targets outside the brain that have been tested in trials or are now approved for clinical use.[15-18] MRI guidance has also been demonstrated for laser thermal ablation in the brain.[2,3,19]

Despite these developments, the cranium has been an obstacle for the use of focused ultrasound in the brain. In the first focused ultrasound trials,[12,13] the ultrasound exposures (sonications) were performed through a craniotomy, making a noninvasive procedure invasive and substantially less desirable. For this reason, only a few other clinical trials in the brain have been attempted.[20-24]

Transcranial application of focused ultrasound has been prevented because of the interaction of the cranium on the ultrasound propagation. Acoustic attenuation in bone, which is approximately 30 to 60 times higher than in soft tissue, causes rapid heating in the cranium and limits the exposure levels that can be safely applied. We have proposed a solution to this problem in which a hemispherical transducer operating at a lower frequency is used to generate the ultrasound beam and the scalp is actively cooled.[25,26] The lower ultrasound frequency reduces absorption in the cranium, and the hemispherical design distributes the resulting bone heating over a large enough area to prevent overheating. Its large geometric aperture also increases the gain of the transducer and permits sufficient focal intensity to allow ablation even at lower frequencies. Simulations and experiments suggest that an optimal ultrasound frequency to balance the cranium and focal heating is approximately 700 kHz,[27] lower than the 1 to 4 MHz commonly used in other targets.

Although lower frequency ultrasound and a hemisphere design can mitigate bone heating, the cranium also has a huge effect on the beam propagation. It is sometimes possible to focus an ultrasound beam through some locations in the cranium,[28] but variations in cranial shape and thickness make it impossible to achieve such focusing reliably without some sort of correction. These aberrations can be corrected using an array of a large number of transducers to tailor the beam propagation.[29,30] With individual driving hardware for each element of this array, one can apply phase offsets to correct for delays in the wave propagation at each location in the cranium. The patient-specific corrections required for each element of this phased array can be determined using acoustic simulations combined with the geometric and density information obtained from computed tomography (CT) scans of the cranium acquired before treatment.[31,32] Phase offsets can also be used to steer the focal position electronically, and modification of the amplitude of each element can normalize the ultrasound intensity across the brain surface.

Based on extensive preclinical acoustic[25-27,29,32-35] and MRI[36-39] studies, a clinical prototype of a phased-array transcranial MRI-guided focused ultrasound surgery (TcMRgFUS) device for thermal ablation was developed.[40-42] Here we present initial technical results of this device from patient treatments, demonstrating the feasibility of focusing through the cranium and measuring the temperature increase at the focus and on the brain surface using MRI. Detailed clinical findings will be presented at a later date at the completion of the study.

PATIENTS AND METHODS

Patients

The treatments were approved by our local institutional review board, and we obtained informed consent. Three men (ages 47, 23, and 34 years) with glioblastoma were treated with TcMRgFUS as part of a phase I clinical trial at our institution testing feasibility and safety. All 3 patients were treated with chemotherapy and radiation therapy before TcMRgFUS, and surgery was not offered as an option by the referring neurosurgeon. Inclusion criteria allowed treatment of adult patients (ages 18–70 years) with either inoperable recurrent glioblastoma (grade IV on the American Society for Therapeutic Radiology and Oncology scale) or recurrent metastatic cancer to the brain with defined margins on contrast MRI. Eligibility requirements included limitations on tumor number, size, and location; patient health; and medical history. Patients unable to undergo an MRI examination, unable to communicate sensations to the treatment team during TcMRgFUS, with extensive changes to 30% or more of the cranium or scalp from disease or previous surgery, with surgical clips or devices in the cranium or brain, unable to attend all study visits (i.e., life expectancy less than 3 months), with evidence of recent (less than 2 weeks before TcMRgFUS) hemorrhage, or who anticipated alternative treatments within 30 days were excluded from the trial. Before treatment, the head was shaved, and the patient lay supine on the treatment device, which was integrated into a standard MRI table. The patient's head was stabilized using a thermoplastic mask designed for radiotherapy (Med-Tec, Orange City, Iowa) with minor mechanical adaptations to the patient interface. They were awake during the procedure, but under intravenous conscious sedation and were instructed to inform the team if any pain was present during sonication. The patient, anesthesiologist, and the TcMRgFUS operator also had access to a button that when pressed would immediately stop any sonication in case of pain. The patient's vital signs were monitored throughout treatment by the anesthesiologist, who remained in the MRI room throughout the procedure. Core body temperature was maintained using a heated blanket (Bair Hugger model 750, Arizant, Eden Prairie, MN).

Device

The treatments were performed using the ExAblate 3000 TcMRgFUS system (InSightec, Haifa, Israel), which consists of a 30-cm diameter hemispherical 512-element phased-array transducer operating at 670 kHz coupled with a 512-channel driving system, a treatment planning/MRI thermometry/dosimetry workstation, and a water cooling/circulation/degassing system. The system was integrated with a clinical 1.5-T MRI unit (General Electric Medical Systems, Milwaukee, WI). The system allowed individual control of the phase and amplitude for each element

in the phased array. The maximum total acoustic power applied was 650 W for patient 1 and was increased to 800 W for patients 2 and 3. The lower value for patient 1 resulted from a conservative software setting. Calibration of the device was performed by the manufacturer. The width and length of the half-intensity profile produced by the transducer in water were 2 and 4 mm, respectively. MRI was performed using the body coil.

The transducer was oriented on its side and was housed in a manually operated positioning system with 6 degrees of freedom (xyz translation, 3 angles) that was integrated into a standard MRI table. This positioning system was used to place the geometric focus of the transducer on the center of the planned tumor target; additional focal steering was achieved using electronic steering via the phased array. The location and orientation of the transducer in the MRI space were monitored throughout treatment using 4 small MRI tracking coils embedded as part of the transducer housing. The 512-channel driving system was located inside the MRI room. A control computer and power supply as well as the water cooling/circulation/degassing system and the treatment planning/ MRI thermometry/dosimetry workstation were located outside the room. Figure 1 shows a diagram of the system.

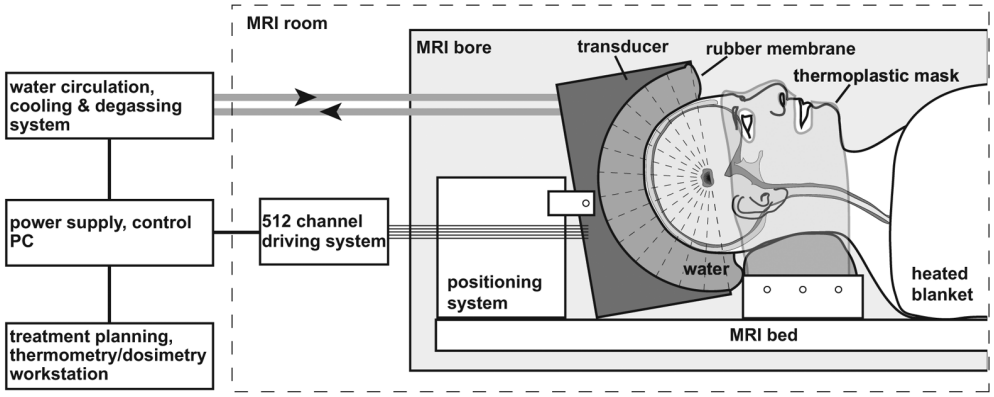

FIGURE 1. *Diagram of the transcranial magnetic resonance imaging–guided focused ultrasound surgery device for noninvasive brain tumor ablation.*

A circular flexible membrane was used to contain the water that filled the space between the transducer and the head. This membrane had a hole cut in it that was stretched around the patient's head. The hole was tight enough to prevent water from leaking out, but not so tight as to cut off blood flow to the scalp. The membrane's outer circumference was sealed to the outside face of the transducer. The water allowed acoustic coupling of the ultrasound beam and cooled the scalp to reduce the risk of thermal damage resulting from cranial heating. This water was chilled to 15 to 20°C and was circulated between sonications. Water temperature and pressure inside the transducer were monitored throughout treatment.

The treatment planning software was used to provide phase offsets to compensate for cranium-induced beam aberrations based on CT scans showing the geometry and density of the cranium. For each transducer element with an angle between it and the cranial surface less than 45 degrees, an algorithm similar to that presented by Clement and Hynynen[32] was used to add a phase offset to correct for the effect of the bone. This offset was determined by the average thickness and density of the cranium in the path of the element.[33] For angles 45 degrees or greater, total reflection was assumed[43] and the element was deactivated. The relationship between the density measured on the CT scan and the speed of sound was that found experimentally in ex vivo human crania.[33] The amplitude of each element was modulated to obtain an equal acoustic intensity on average at the brain surface.

TcMRgFUS Treatment

Before treatment, the patient underwent a CT scan (512 × 512 matrix, 1-mm slice thickness) that covered the entire cranium and MRI with contrast (0.1 mmol/kg Magnevist [gadopentetate dimeglumine]; Berlex Laboratories, Wayne, NJ) obtained with the patient in place in the device (without water). Axial, sagittal, and coronal T2-weighted fast spin echo images and contrast-enhanced T1-weighted images were used to define the tumor volume for treatment planning. During this imaging session, the thermoplastic mask was fit to the patient, and the position and angle of the transducer were set by the manual positioning system so that the geometric focus was located in the center of the target volume and the transducer beam path covered as large a surface area on the cranium as possible. These images were used to prescribe a detailed treatment plan that was used on the following day. The different imaging sets were registered to each other and to the current MRI/transducer coordinates using volumetric registration algorithms developed as part of ExAblate 3000 software tools.[44] The CT scan was used in acoustic models by the TcMRgFUS software to correct for ultrasound beam aberrations. It covered the entire head instead of only the portion over which the ultrasound beam passed to facilitate its registration with subsequent MRI scans.

On the treatment day, the patient and TcMRgFUS device were prepared as described, and axial, sagittal, and coronal T2-weighted fast spin echo images were acquired. These images were registered to the previously acquired CT and magnetic resonance images, and the treatment plan was displayed (Fig. 2). This registration was verified visually by the operator by displaying the cranium (automatically segmented in the CT scan) as a colored overlay on the MRI scans. Registration errors were corrected using a graphical tool integrated in the planning software. The individual beam paths were also displayed on top of the images, allowing any element to be deactivated if its path passed through unwanted locations, which in these patients were burr holes and sites of previous surgical resection. After this plan was completed, sonication began.

The acoustic power was slowly increased over several 20-second sonications until focal heating was observed in MR temperature imaging (MRTI) to verify the target location within the tumor. After such verification, the acoustic power was increased further over additional 20-second sonications. The goal was to achieve a sufficient thermal dose[45] to achieve thermal coagulation, approximately 55°C peak temperature or 240 equivalent minutes at 43°C.[46] However, as described below, we were limited by the device's maximum acoustic power level (650 W in patient 1, 800 W in patients 2 and 3) and by pain in patient 3.

For MRTI, phase-difference images of a fast spoiled gradient echo sequence were obtained to estimate changes in the temperature-sensitive water proton resonant frequency.[14] The following parameters were used for MRTI: TR/TE, 38/19 ms; flip angle, 30 degrees; slice thickness, 3 to 5 mm; field of view, 28 cm; matrix (frequency × phase), 256 × 128; band-

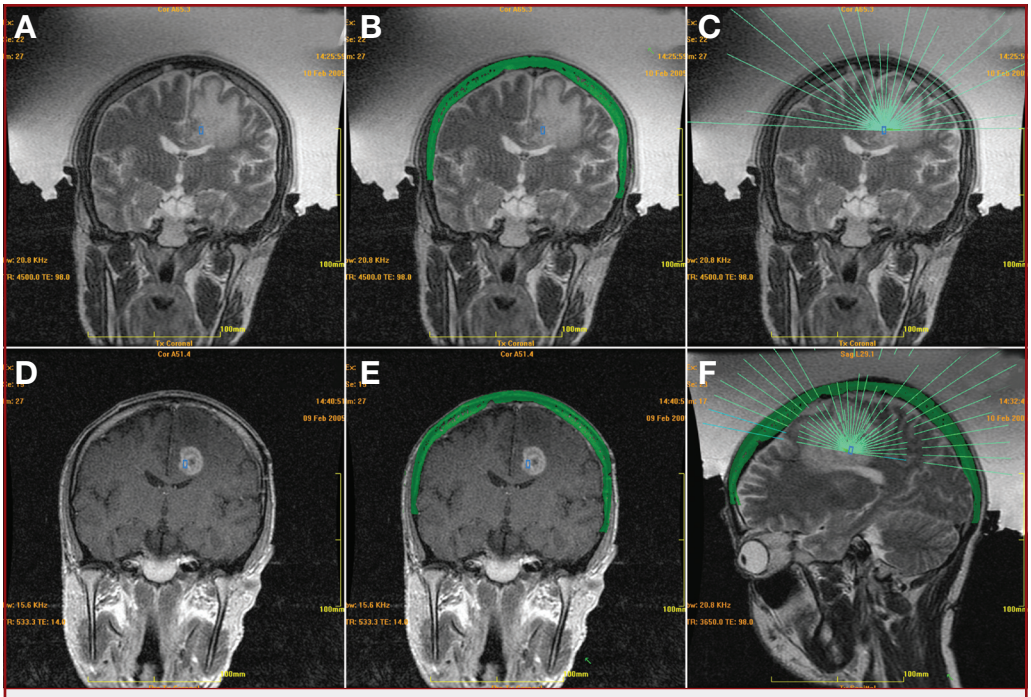

FIGURE 2. *Screenshots from transcranial magnetic resonance imaging–guided focused ultrasound surgery (TcMRgFUS) treatment planning workstation.* **A**, *coronal T2-weighted images of the patient in the TcMRgFUS device. The target of the current sonication is indicated by the blue rectangle. The water filling the space between the patient's shaved head and the transducer can be seen.* **B**, *Pretreatment computed tomography (CT) scan data of the cranium is registered the intratreatment magnetic resonance imaging (MRI) scans. The cranium is automatically segmented from the CT scan and displayed on top of the magnetic resonance images used for treatment planning as a green region. Any registration errors can be seen on these images and corrected by the user by using a graphical tool. Magnetic resonance tracking coils integrated into the transducer are used to register the TcMRgFUS system coordinates with the imaging coordinates. Acoustic models taking into account the patient-specific cranium geometry and density are used to correct for aberrations to the ultrasound beam.* **C**, *the beam paths for each phased-array element are superimposed on the images, allowing the user to verify that no beams pass through undesired structures.* **D** *and* **E**, *pretreatment contrast-enhanced T1-weighted images, which can be useful to define tumor margins, acquired the day before treatment can also be registered to the intratreatment images. Axial and sagittal images are also acquired, allowing for treatment planning in 3 dimensions.* **F**, *sagittal T2-weighted image.*

width, ±3.57 kHz; scan time, 5 seconds. A time series of images in a single, user-defined plane were obtained before, during, and after each sonication. The scanner reconstructed complex image data needed to create these phase-difference images, which were converted to temperature maps by the treatment planning/MRI thermometry/dosimetry workstation using a temperature sensitivity of –0.01 ppm/°C.[47] Estimates of absolute temperatures assumed a 37°C baseline tissue temperature.

Posttreatment Analysis

Posttreatment data analysis was performed by 1 author (N.M.) using software written in Matlab (version 7.4; The Mathworks, Natick, MA). The maximum temperature increase achieved at each visible focal hot spot was calculated and compared with the heating on the outer brain surface induced by ultrasound absorption in the cranium. To combine the results of the different sonications, which were performed at different exposure levels, we normalized the temperature increase to the applied acoustic power, a valid assumption for linear acoustic propagation.[48]

Although the ultrasound intensity outside the focal region is expected to be insufficient to produce direct heating of brain tissue, the cranium will heat appreciably because of high acoustic absorption and, as a result, will heat the brain surface. Because cranium-induced brain surface heating will be a major limiting safety factor for TcMRgFUS, the temperature changes in this area were carefully examined using the following procedure. First, the entire brain was manually segmented in the magnitude fast spoiled gradient echo images used for the MRTI, excluding areas between the brain surface and cranium containing cerebrospinal fluid. The outer brain surface within the transducer path was then identified. A range of 3 or more consecutive temperature images were also identified near the end of the time series of the MRTI where the brain surface temperature seemed to reach a steady state and were free of phase artifacts that persisted after application of the correction scheme described below. These persistent artifacts were manifested by temporal jumps in temperature that were clearly inconsistent with expected heating. Brain surface heating was measured on coronal and sagittal images; axial images were excluded because the cranium was not necessarily normal to the image plane, and partial volume effects could dominate. Temperature measurements within the cranium were not possible because of a lack of magnetic resonance signal in bone.

Two procedures were used to quantify the brain surface heating. In the first, the overall mean surface heating was calculated in a 2-voxel wide strip at the brain surface. In the second, a conservative (worse-case) metric that attempted to take into account nonuniform heating was devised. The mean temperature increase of the hottest 5% of the voxels within 6 to 7 voxels (approximately 7 mm) of the outer brain surface was identified. To minimize bias to noise or artifacts unrelated to temperature, these voxels were identified on the averaged map of 3 or more images at the end of the MRTI time series when the heating reached steady state and the region defined by these voxels was extended by 1 voxel in every direction. These criteria were determined ad hoc with an aim of including only the hottest voxels but with a sufficient number to average out noise or other temperature measurement artifacts, which were assumed to be randomly distributed around zero. Brain surface heating values quoted in the following are the average of 3 or more images where the temperature increase seemed to stabilize.

Phase instabilities in the MRTI were corrected in the posttreatment analysis using nonheated brain areas. To define these areas, the segmentation of the brain surface was eroded at the edges by 6 to 7 voxels (approximately 7 mm) and a circular 1-cm region of interest (ROI) surrounding the focal target was excluded. Voxels within ventricles were also excluded

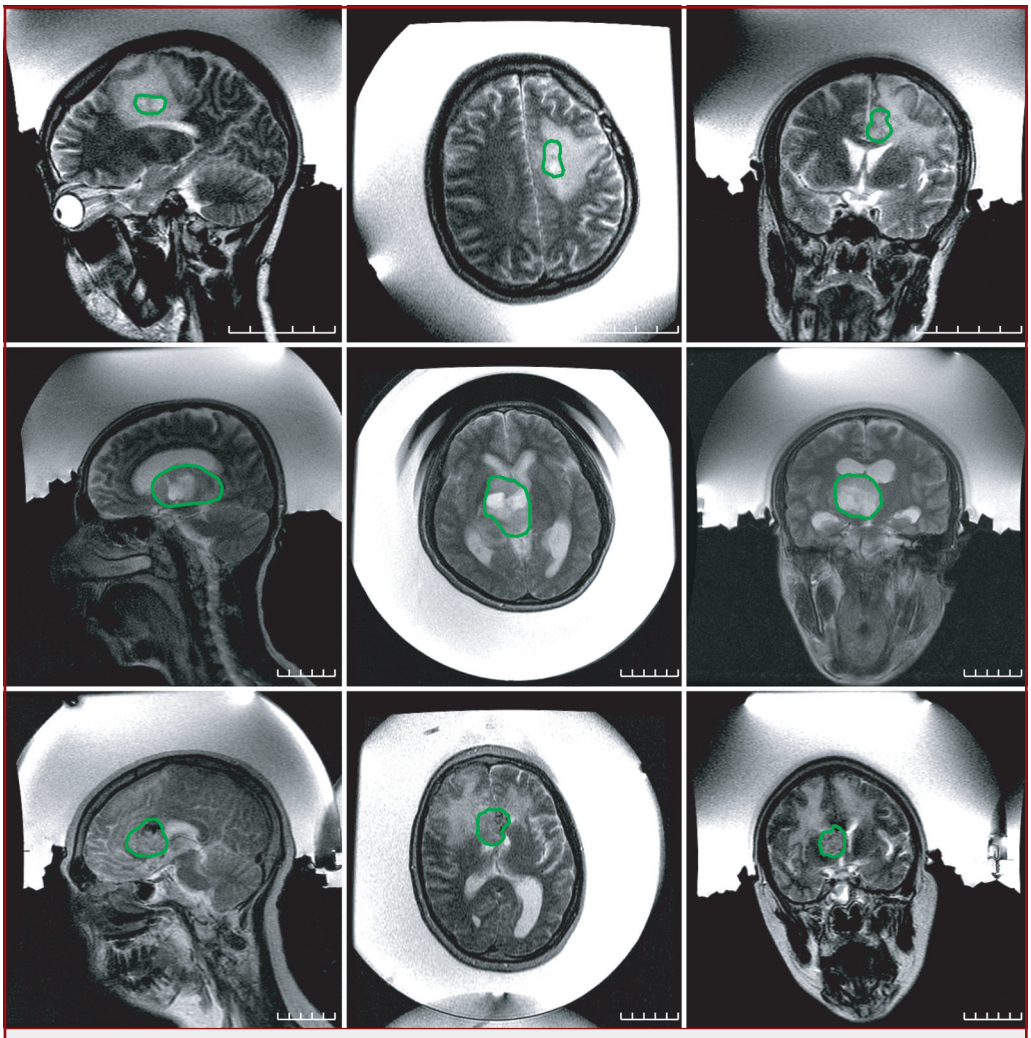

FIGURE 3. *T2-weighted fast spin echo images of the patients in the transcranial magnetic resonance imaging–guided focused ultrasound surgery device. The outlines approximately delineate the boundaries of the targeted tumors. The space between the patients' shaved heads and the hemispherical transducer was filled with chilled water that was continuously degassed and circulated before and between sonications. Patient 1 (top), patient 2 (middle), patient 3 (right); sagittal images (left), axial images (center), coronal images (right).*

because they had uncorrelated phase artifacts resulting from fluid flow, presumably resulting from acoustic streaming. The phase-difference distribution in the remaining nonheated/nonventricular voxels was then fit to a nonspecific smooth surface using a regularized, piecewise linear (low-order spline) surface model. The regularization is based on the Laplacian of the surface and is used to penalize deviations from smoothness in the fitted surface. This surface fit of the artifact was then extrapolated into the heated regions at the focal point and outward to the brain surface and subtracted off. The ability of this method to correct for phase instabilities was tested by repeating this procedure in a separate 1-cm ROI in a nonheated area instead of the focal point and verifying that its average phase offset approached zero. We could not verify the correction algorithm in this way on regions at the brain surface because no images were obtained without potential heating. The noise level in the MRTI was found by calculating the average standard deviation in the nonheated regions of interest used to test the correction scheme. Separate noise estimates were obtained for images acquired during and after sonication. The maximum temperature increases per watt at the focus and on the brain surface were compared using an unpaired *t* test. Differences between the 2 metrics for brain surface heating estimates were compared using a paired *t* test.

RESULTS

The T2-weighted fast spin echo images of the 3 patients within the TcMRgFUS device are shown in Figure 3. The location of the target tumors in the thalamus was relatively deep and central within the brain. The cranial area over which the acoustic beam was distributed was calculated by the treatment planning workstation to be 284, 327, and 354 cm^2, for patients 1 to 3, respectively. The highest acoustic power level attempted in patient 1 was 650 W, which was the maximum value available for that treatment because of a conservative software setting. The maximum acoustic power available for the other patients was 800 W. This level was achieved in patient 2, but in patient 3, sonication-related pain was reported at 650 W, and higher values were not tested. Pain related to the thermoplastic mask and neck support limited the treatment time available. Comparison of pre- and post-TcMRgFUS images showed that small patient motion (approximately 2–4 mm) occurred over the course of the treatment.

Focal heating was readily observed within the target tumor in MRTI during 3 of 12, 14 of 16, and 11 of 17 of the sonications delivered in patients 1 to 3, respectively. The overall maximum focal temperature achieved during a 20-second sonication was approximately 51°C, near but not clearly above the threshold for thermal damage in the brain.[38] Individually, the maximum temperature achieved was 42, 51, and 48° C, for patients 1 to 3, respectively. Changes resulting from treatment were not evident in the tumor, surrounding brain, or brain surface in post-TcMRgFUS MRI performed immediately after the procedure. No skin burns were observed after treatment, and no skin pain was reported.

The resulting maximum estimated average acoustic intensity on the outer cranial surface for the 3 patients was 2.8, 2.5, and 1.8 W/cm^2, respectively. The maximum temperature increases in the hottest regions within 7 mm of the brain surface were 2.5, 3.8, and 2.4°C in patients 1 to 3, respectively. This result represents a conservative estimate of brain surface heating that allowed for hot spots at discrete locations but that was also potentially sensitive to bias. When considering all voxels within a 2-voxel wide strip at the edge of the brain surface, the maximum measured brain surface temperature increase resulting from cranial heating was 0.9, 1.5, and 1.2°C in patients 1 to 3, respectively. Overall, the temperature increase on the brain surface per average watt per square centimeter on the outer cranial surface (estimated by TcMRgFUS software) was 1.3 ± 0.3 and 0.5 ± 0.2°C/W/cm^2, for the 2 metrics tested. Figure 4 shows examples of the focal and cranial heating observed in the MRTI. No heating other than at the focus and on the brain surface was observed.

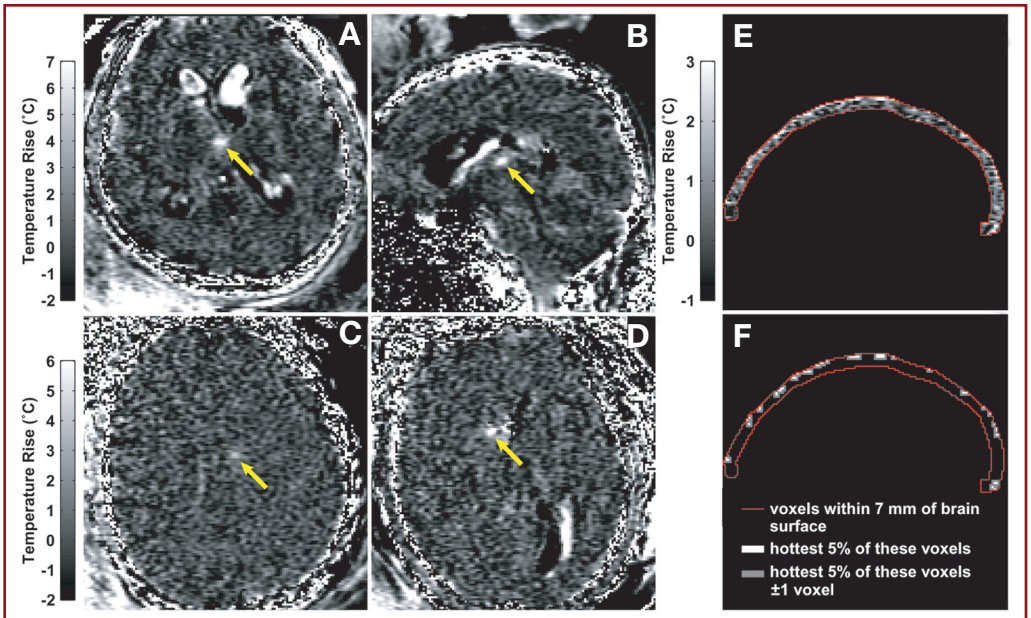

FIGURE 4. *Focal heating (arrows) during transcranial magnetic resonance imaging–guided focused ultrasound surgery in the 3 patients. Sagittal (**A**) and axial (**B**) examples of magnetic resonance temperature imaging (MRTI) acquired at peak temperature increase during two 20-second sonications (acoustic power, 800 W) in patient 2. Axial MRTI showing focal heating in patients 1 (**C**) and 3 (**D**), respectively (acoustic power, 650 W and 594 W, respectively). The focus in patient 3 was located close to a region containing blood products from a previous biopsy, which caused signal loss and artifact in the MRTI. Flow of the fluid in the ventricles produced phase instabilities that resulted in the white and black areas evident in the brain away from the focal spot that can be seen in **A**, **B**, and **D**. Images shown at native resolution. Areas with low-magnitude signal produced white noise in the phase-difference images used for MRTI that are evident in the cranial bone and at the image periphery. **E**, heating on the brain surface by the acoustic absorption in the cranium at the end of the MRTI acquisition resulting from a 20-second sonication in patient 3 (acoustic power, 491 W). The heating was quantified by searching for the hottest voxels in the displayed 6- to 7-voxel wide strip in a composite image that was the average of 3 or more temperature maps acquired when the brain surface temperature was at steady state. **F**, the location of the hottest 5% of the voxels in this strip ±1 voxel that were used to provide a conservative estimate of the brain surface heating.*

When normalizing all the measurements to the applied acoustic power, the average ratio between the focal heating and that of the hottest voxels near the brain surface induced by cranial heating was 4.0 ± 1.7; the mean ratio between the focal heating and that of the 2-voxel wide strip at the brain surface was 10.5 ± 5.5. The mean normalized temperature increase per watt (± standard deviation) at the focus and at the brain surface (using both criteria) for all sonications are plotted in Figure 5. As expected, the focal temperature increase peaks at the end of the 20-second sonication and then cools in subsequent images, whereas the brain surface continues to heat past 20 seconds as the cranium continues to heat the adjacent brain surface via thermal conduction. The peak temperature increase per acoustic watt at the focus was significantly greater than that achieved on the brain surface ($P < 0.01$). The peak brain surface temperature increase estimated using the hottest voxels was significantly greater ($P < 0.01$) than that estimated using the 2-voxel wide strip at the edge of the brain.

Severe instabilities that were observed in the phase difference images used for MRTI (Fig. 6*A*) were subtracted off by fitting the nonheated regions of the brain to a smooth surface (Fig. 6*B*) and extrapolation (Fig. 6*C*). The correction scheme seemed to robustly correct the phase artifacts, as evidenced by analysis of nonheated ROIs substituted for those used around the focus (Fig. 6*D*). Before correction, the average root mean square phase error in test locations was 1.9 ± 3.4°C; after correction, this value was 0.3 ± 0.2°C. The average standard deviation inside these nonheated ROIs, reflective of the image signal-to-noise ratio, was ±1.3 ± 0.4°C. It increased to ±1.6 ± 0.6°C during sonication. A signal void, presumably caused by blood products from a previous biopsy, in a large part of the tumor in patient 3 limited the use of MRTI in that region (Fig. 6*E*).

DISCUSSION

The study demonstrated for the first time that a therapeutic ultrasound beam can be focused in the brain noninvasively through the intact cranium in patients. Although sufficient power was not available to us to clearly achieve thermal coagulation and significant hurdles remain, these findings are a major step forward in producing a completely noninvasive alternative to surgical resection for brain disorders. As described in the following, based on these

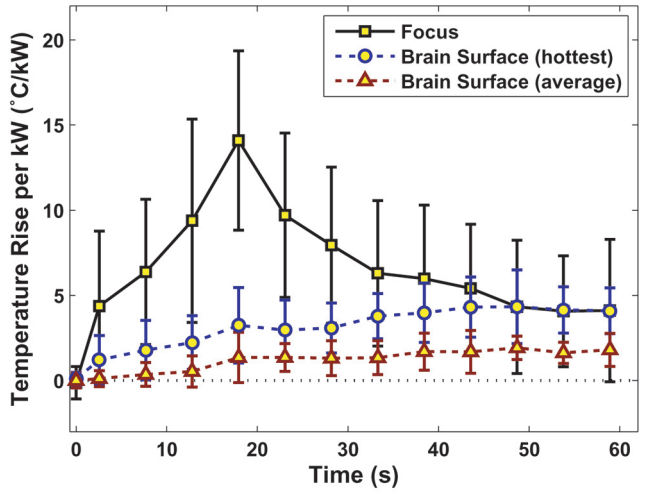

FIGURE 5. *Temperature increase normalized to the applied acoustic power as a function of time at the focus and on the brain surface as measured by magnetic resonance temperature imaging (MRTI). The brain surface was heated by the cranial bone, which is highly absorbing of ultrasound. Two metrics were tested to measure the temperature on the brain surface. The first aimed to be a conservative (worse-case) metric that identified any hot spots at particular locations and considered the hottest voxels within 6 to 7 voxels of the brain surface. The second measured the mean temperature increase of all voxels within a 2-voxel wide strip at the brain surface. Mean ± standard deviation shown of 28 sonications for focal heating, 15 for brain surface heating. The data showing the temperature at the focus are from all sonications in the 3 patients in whom focal heating was observed on MRTI; the brain surface heating was from all sonications in the 3 patients in whom sagittal or coronal MRTI was used.*

findings, it seems that TcMRgFUS ablation of brain tumors will be feasible with this device. If this result is verified, a noninvasive alternative to surgical resection could be available to patients, potentially reducing side effects of surgery and providing a treatment options for patients with inoperable tumors. It could also provide an alternative to radiosurgery or a treatment option for patients with recurrence after radiotherapy.

These treatments were in patients with inoperable glioblastoma, which may not ultimately be the best clinical target for TcMRgFUS because of its infiltrative nature. This treatment is a noninvasive alternative to surgical resection. Although it offers a major reduction in side effects, it is known that surgery offers only limited improvement in survival for these patients. We anticipate that better targets for TcMRgFUS will be those for which surgical resection currently offers greater benefit, such as metastases or other tumors with well-defined margins and benign tumors. One may ultimately be able to improve on surgical resection with TcMRgFUS by taking advantage of the synergistic effects of heat with radiation therapy or chemotherapy.

Extrapolation of the mean focal temperatures and a conservative estimate of cranium-induced heating achieved during these treatments suggest that with sufficient power, one could achieve thermal coagulation at the focus without overheating the brain surface. For example, the average measurements at the focus suggest that to achieve a peak focal temperature of 55°C, which would be sufficient to produce thermal necrosis, would require approximately 1200 W of acoustic power for a 20-second sonication. At this value and assuming a baseline temperature of 37°C, our measurements suggest that the brain surface would heat to approximately 39 to 42°C, which is below the thermal damage threshold for the relatively short heating durations used with TcMRgFUS. Other effects have been observed for low-level heating for longer heating durations, such as necrosis[49] and febrile seizures.[50,51] One needs to consider the risk of such effects resulting from the cumulative thermal dose on the brain surface when multiple sonications are used to treat a tumor volume.

The mean brain surface temperature per watts per square centimeter on the brain surface was lower than measured in preclinical animal tests. In primate tests,[42] the mean temperature increase across the brain surface was 2.6 ± 0.2°C/ W/cm^2, with the hottest voxels giving an average value of 4.0 ± 0.2°C/W/cm^2. In similar pig experiments,[37] the average brain surface heating was observed to be 2.2 ± 0.5°C/W/cm^2. Differences can be explained by differences in cranial thickness and densities in the animal models.

These results, along with sonication-related pain that occurred in patient 2, suggest that the safety window seems to be relatively narrow and could limit the extent of the brain that can be targeted with this device without overheating the cranium. The locations of these patients' tumors, relatively deep and centrally located, were nearly optimal for this device with respect to cranial heating. Such locations allow the ultrasound beam to be distributed over a large portion of the cranium and result in nearly normal angles between most of the array elements and the cranium. For tumors that are not centered in this way, the angles between the cranium bone and the transducer face would deviate from normal, resulting in nearly complete reflection for many elements. Deactivation of those elements would result in a smaller portion of the transducer surface being active and higher local ultrasound intensities on the cranium. Despite these limitations, the device seems to be capable of noninvasively ablating deep and centrally located tumors, locations where surgery is challenging or not an option. It may also be useful for noninvasive functional neurosurgery in which many targets are deep within the brain. The source of the sonication-related pain in 1 patient is not known. We suspect that the pain resulted from heating of the dura. It is possible that the dura extended into the brain midline in this patient and was perhaps close to the focal zone.

To improve the targetable locations in the brain, the manufacturer has made substantial changes to the device and treatment strategy to be used in subsequent patient treatments in this trial.[52] These changes include doubling the number of elements in the phased array, increasing the maximum available power, lowering the ultrasound frequency, and taking advantage of bubble-enhanced absorption to boost the focal heating.[53] The thermoplastic mask has also been replaced by a standard stereotactic surgery device with pins to prevent motion and discomfort. This motion resulted in long treatments (because of a need to repeat the treatment plan-

ning) and may have caused error in the aberration correction and in the MRTI. Results of treatments with this new version of the TcMRgFUS system will be presented separately.

We should note that several factors potentially resulted in an underestimation of the ratio of focus to brain surface heating. Because the design of this prototype device precluded the use of an imaging coil, the body coil was used for the imaging, and a 3- to 5-mm slice thickness was necessary to achieve marginally acceptable MRTI. Volume averaging (i.e., the partial volume effect), especially if the focal spot was not centered on the slice, likely resulted in an underestimation of the maximum temperature achieved. In addition, the small patient motion that was observed over the course of the treatment could have degraded the aberration correction, resulting in suboptimal focusing. Furthermore, our method to conservatively estimate the brain surface heating was susceptible to some bias, resulting from noise and/or phase instabilities that were not corrected, potentially resulting in an overestimate of the cranium-induced heating. Finally, it could be that the cooling of the scalp during treatment could actually decrease the brain surface temperature, which would increase the safety window.

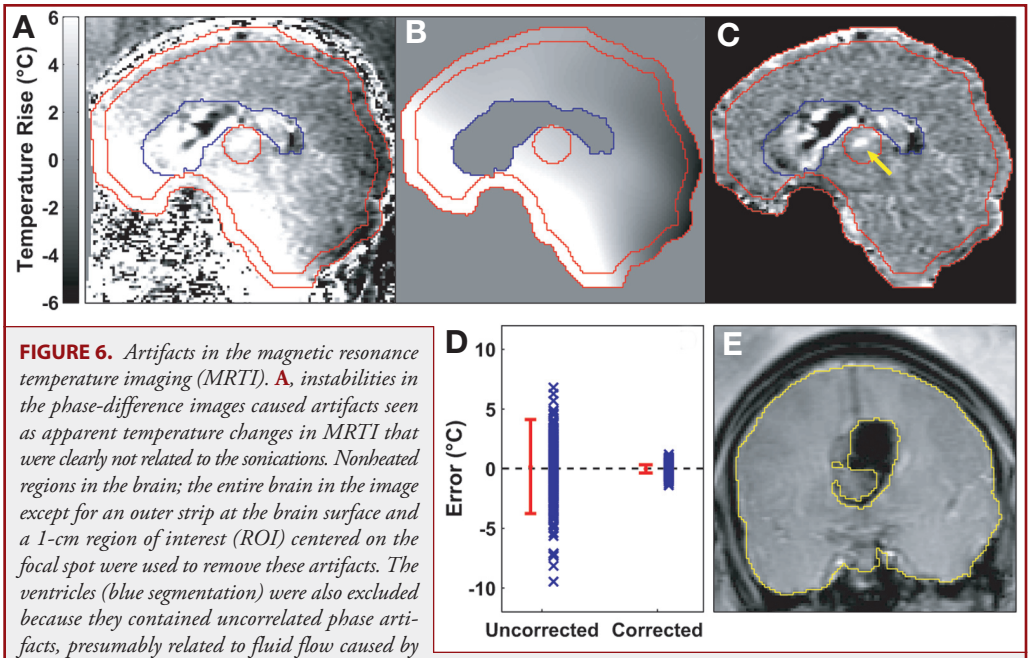

FIGURE 6. *Artifacts in the magnetic resonance temperature imaging (MRTI).* **A**, *instabilities in the phase-difference images caused artifacts seen as apparent temperature changes in MRTI that were clearly not related to the sonications. Nonheated regions in the brain; the entire brain in the image except for an outer strip at the brain surface and a 1-cm region of interest (ROI) centered on the focal spot were used to remove these artifacts. The ventricles (blue segmentation) were also excluded because they contained uncorrelated phase artifacts, presumably related to fluid flow caused by acoustic streaming.* **B**, *the phase difference in the nonheated regions were fit to a smooth surface and extrapolated into the heated regions.* **C**, *this surface was then subtracted from the phase-difference image.* **D**, *this correction was tested by repeating the procedure using a region of interest (ROI) in a nonheated brain area instead of that surrounding the focal point and verifying that after correction, the mean apparent temperature change was zero. The plot shows temperature error in these ROIs in all the individual temperature maps acquired during all 45 sonications before and after the correction.* **E**, *in patient 3, a large signal void in the images used to create the MRTI prevented temperature measurement in a large proportion of the tumor. The magnitude reconstruction of the gradient echo sequence used for MRTI is shown.*

A major limitation of the study was our inability to achieve ablation in these patients. Previous tests with this device sonicating in vivo tissue in rabbits through a human cranial sample were able to create thermal lesions. In that study, focal temperature changes of 22 ± 10°C/kW were achieved,[41] which were greater than the average value of 15.5 ± 5.1°C/kW in these treatments. This difference was likely attributable to the human treatments being at deeper tissue locations and the difference between ultrasound absorption and blood perfusion in the normal rabbit brain and human tumors. We might have been able to achieve ablation in our patients if we had used longer sonications or performed additional sonications to accumulate the thermal dose past the damage threshold at the focal spot. However, because of long treatment times, patient discomfort caused by the thermoplastic mask, and our desire to be conservative in these first treatments, such additional exposures were not attempted.

Another limitation of this study was the quality of the MRTI. The noise level was only acceptable using a 3- to 5-mm slice thickness, and it increased during sonication. Future device designs would benefit greatly from integration of an imaging coil to allow multiple, thinner image planes with better in-plane resolution for the MRTI and better electrical isolation of the TcMRgFUS hardware to reduce sonication-related noise. The large phase instabilities observed in the MRTI were also problematic. Although similar artifacts were reported in other work resulting from patient motion or magnetic field instabilities, we did not expect them to occur in the brain with this system in which the head is fixed in place. The source of these instabilities, although not clear, were potentially caused by magnetic field changes caused by blood flow or brain pulsation, or, more likely, motion of the mouth and tongue or other body parts outside of the brain during sonication. We do not suspect that they were produced by the TcMRgFUS system (such as from water motion) or from instabilities in the MRI itself because they were not observed in preclinical tests with this device.[40-42] Our correction algorithm seemed to successfully remove the phase instabilities overall, but future work will be needed to validate it. Although analysis of the method using dummy (nontargeted) locations suggests that it can robustly correct errors in ROIs within the brain, sometimes the instabilities seemed to remain after correction at the brain surface. This might be expected because the extrapolation of the fit surface of the artifact at the edges is based on less information than at ROIs within the brain that are completely surrounded.

An additional problem occurred in patient 3, in whom signal loss in the MRTI, presumably resulting from blood products remaining from a previous intervention, prevented us from mapping the temperature changes in a substantial portion of that tumor. This loss was presumably caused by T2* shortening caused by magnetic susceptibility differences. If methods cannot be developed to compensate for such artifacts, they could pose a limitation to this technology in these cases. In particular, many high-grade gliomas as well as melanoma and renal cell carcinoma metastases have such blood products that may cause difficulty with the MRTI.

CONCLUSION

This work showed for the first time that ultrasound can be focused through the intact cranium in patients and that the heating can be visualized using MRTI. Although device power limited our ability to achieve thermal coagulation, extrapolation of the results suggests that ablation will be possible without overheating the cranium. Analysis of the brain surface heating and the occurrence of sonication-related pain in 1 patient suggest, however, that the targetable regions of the brain may be limited to deep, central locations in the brain with the device.

Disclosure

Two authors (KH and FAJ) served in the past as consultants to InSightec. The other authors have no personal financial or institutional interest in any of the drugs, materials, or devices described in this article.

REFERENCES

1. Anzai Y, Lufkin R, DeSalles A, Hamilton DR, Farahani K, Black KL. Preliminary experience with MR-guided thermal ablation of brain tumors. *AJNR Am J Neuroradiol.* 1995;16:39-52.
2. Kahn T, Bettag M, Ulrich F, et al. MRI-guided laser-induced interstitial thermotherapy of cerebral neoplasms. *J Comput Assist Tomogr.* 1994;18:519-532.
3. Kettenbach J, Kuroda K, Hata N, et al. Laser-induced thermotherapy of cerebral neoplasia under MR tomographic control. *Min Invas Ther Allied Technol.* 1998;7:589-598.
4. Lynn JG, Zwemer RL, Chick AJ, Miller AE. A new method for the generation and use of focused ultrasound in experimental biology. *J Gen Physiol.* 1942;26:179-193.
5. Barnard JW, Fry WJ, Fry FJ, Krumins RF. Effects of high intensity ultrasound on the central nervous system of the cat. *J Comp Neurol.* 1955;103:459-484.
6. Fry WJ, Brennan JF, Barnard JW. Histological study of changes produced by ultrasound in the gray and white matter of the central nervous system. *Ultrasound Med Biol.* 1957;3:110-130.
7. Astrom KE, Belle, Ballantine HT Jr, Heidensleben E. An experimental neuropathological study of the effects of high-frequency focused ultrasound on the brain of the cat. *J Neuropathol Exp Neurol.* 1961;20:484-520.
8. Ballantine HT Jr, Hueter TF, Nauta WJ, Sosa DM. Focal destruction of nervous tissue by focused ultrasound: Biophysical factors influencing its application. *J Exp Med.* 1956;104:337-360.
9. Lele PP. A simple method for production of trackless focal lesions with focused ultrasound: Physical factors. *J Physiol.* 1962;160:494-512.
10. Vykhodtseva NI, Gavrilov LR, Mering TA, Iamshchikova NG. Use of focused ultrasound for local destruction of different brain structures [in Russian]. *Zh Nevropatol Psikhiatr Im S S Korsakova.* 1976;76:1810-1816.
11. Warwick R, Pond J. Trackless lesions in nervous tissues produced by high intensity focused ultrasound (high-frequency mechanical waves). *J Anat.* 1968;102:387-405.
12. Hickey RC, Fry WJ, Meyers R, Fry FJ, Bradbury JT. Human pituitary irradiation with focused ultrasound. An initial report on effect in advanced breast cancer. *Arch Surg.* 1961;83:620-633.
13. Meyers R, Fry WJ, Fry FJ, Dreyer LL, Schultz DF, Noyes RF. Early experiences with ultrasonic irradiation of the pallidofugal and nigral complexes in hyperkinetic and hypertonic disorders. *J Neurosurg.* 1959;16:32-54.
14. Ishihara Y, Calderon A, Watanabe H, et al. A precise and fast temperature mapping using water proton chemical shift. *Magn Reson Med.* 1995;34:814-823.
15. Chapelon JY, Ribault M, Vernier F, Souchon R, Gelet A. Treatment of localised prostate cancer with transrectal high intensity focused ultrasound. *Eur J Ultrasound.* 1999;9:31-38.
16. Sanghvi NT, Foster RS, Bihrle R, et al. Noninvasive surgery of prostate tissue by high intensity focused ultrasound: An updated report. *Eur J Ultrasound.* 1999;9:19-29.
17. Tempany CM, Stewart EA, McDannold N, Quade BJ, Jolesz FA, Hynynen K. MR imaging-guided focused ultrasound surgery of uterine leiomyomas: A feasibility study. *Radiology.* 2003;226:897-905.
18. Wu F, Chen WZ, Bai J, et al. Pathological changes in human malignant carcinoma treated with high-intensity focused ultrasound. *Ultrasound Med Biol.* 2001;27:1099-1106.
19. Jolesz FA, Bleier AR, Jakab P, Ruenzel PW, Huttl K, Jako GJ. MR imaging of laser-tissue interactions. *Radiology.* 1988;168:249-253.
20. Guthkelch AN, Carter LP, Cassady JR, et al. Treatment of malignant brain tumors with focused ultrasound hyperthermia and radiation: Results of a phase I trial. *J Neurooncol.* 1991;10:271-284.
21. Heimburger RF. Ultrasound augmentation of central nervous system tumor therapy. *Indiana Med.* 1985;78:469-476.
22. Oka M, Okumura T, Yokoi H, et al. Surgical application of high intensity focused ultrasound. *Med J Osaka Univ.* 1960;10:427-442.
23. Park JW, Jung S, Junt TY, Lee MC. Focused ultrasound surgery for the treatment of recurrent anaplastic astrocytoma: A preliminary report, in *Therapeutic Ultrasound. 5th International Symposium on Therapeutic Ultrasound*. Melville, NY, American Institute of Physics, 2006, pp 238-240.
24. Ram Z, Cohen ZR, Harnof S, et al. Magnetic resonance imaging-guided, high-intensity focused ultrasound for brain tumor therapy. *Neurosurgery.* 2006;59:949-956.
25. Clement GT, White J, Hynynen K. Investigation of a large-area phased array for focused ultrasound surgery through the skull. *Phys Med Biol.* 2000;45:1071-1083.
26. Sun J, Hynynen K. The potential of transskull ultrasound therapy and surgery using the maximum available skull surface area. *J Acoust Soc Am.* 1999;105:2519-2527.
27. Clement GT, Sun J, Giesecke T, Hynynen K. A hemisphere array for non-invasive ultrasound brain therapy and surgery. *Phys Med Biol.* 2000;45:3707-3719.
28. Fry FJ, Goss SA. Further studies of the transkull transmission of an intense focused ultrasonic beam: Lesion production at 500 kHz. *Ultrasound Med Biol.* 1980;6:33-38.
29. Hynynen K, Jolesz FA. Demonstration of potential noninvasive ultrasound brain therapy through an intact skull. *Ultrasound Med Biol.* 1998;24:275-283.
30. Thomas J, Fink MA. Ultrasonic beam focusing through tissue inhomogeneities with a time reversal mirror: Applicaton to transskull therapy. *IEEE Trans Ultrason Ferroelectr Freq Control.* 1996;43:1122-1129.
31. Aubry JF, Tanter M, Pernot M, Thomas JL, Fink M. Experimental demonstration of noninvasive transskull adaptive focusing based on prior computed tomography scans. *J Acoust Soc Am.* 2003;113:84-93.
32. Clement GT, Hynynen K. A non-invasive method for focusing ultrasound through the human skull. *Phys Med Biol.* 2002;47:1219-1236.
33. Clement GT, Hynynen K. Correlation of ultrasound phase with physical skull properties. *Ultrasound Med Biol.* 2002;28:617-624.
34. Clement GT, Hynynen K. Micro-receiver guided transcranial beam steering. *IEEE Trans Ultrason Ferroelectr Freq Control.* 2002;49:447-453.
35. Connor CW, Clement GT, Hynynen K. A unified model for the speed of sound in cranial bone based on genetic algorithm optimization. *Phys Med Biol.* 2002;47:3925-3944.
36. Hynynen K, Vykhodtseva NI, Chung AH, Sorrentino V, Colucci V, Jolesz FA. Thermal effects of focused ultrasound on the brain: Determination with MR imaging. *Radiology.* 1997;204:247-253.
37. McDannold N, King RL, Hynynen K. MRI monitoring of heating produced by ultrasound absorption in the skull: In vivo study in pigs. *Magn Reson Med.* 2004;51:1061-1065.
38. McDannold N, Vykhodtseva N, Jolesz FA, Hynynen K. MRI investigation of the threshold for thermally induced blood-brain barrier disruption and brain tissue damage in the rabbit brain. *Magn Reson Med.* 2004;51:913-923.

39. Vykhodtseva NI, Sorrentino V, Jolesz FA, Bronson RT, Hynynen K. MRI detection of the thermal effects of focused ultrasound on the brain. *Ultrasound Med Biol.* 2000;26:871-880.
40. Clement GT, White PJ, King RL, McDannold N, Hynynen K. A magnetic resonance imaging-compatible, large-scale array for trans-skull ultrasound surgery and therapy. *J Ultrasound Med.* 2005;24:1117-1125.
41. Hynynen K, Clement GT, McDannold N, et al. 500-element ultrasound phased array system for noninvasive focal surgery of the brain: A preliminary rabbit study with ex vivo human skulls. *Magn Reson Med.* 2004;52:100-107.
42. Hynynen K, McDannold N, Clement G, et al. Pre-clinical testing of a phased array ultrasound system for MRI-guided noninvasive surgery of the brain—a primate study. *Eur J Radiol.* 2006;59:149-156.
43. Clement GT, White PJ, Hynynen K. Enhanced ultrasound transmission through the human skull using shear mode conversion. *J Acoust Soc Am.* 2004;115:1356-1364.
44. Capek M, Mroz L, Wegenkittl R. Robust and fast medical registration of 3d-multi-modality data sets, in *Proceedings of Medicon 2001: IX Mediterranean Conference on Medical and Biological Engineering and Computing*. Zagreb, Croatia, Croatian Society for Medical and Biological Engineering (CROMBES), 2001, pp 515–518.
45. Sapareto SA, Dewey WC. Thermal dose determination in cancer therapy. *Int J Radiat Oncol Biol Phys.* 1984;10:787-800.
46. Meshorer A, Prionas SD, Fajardo LF, Meyer JL, Hahn GM, Martinez AA. The effects of hyperthermia on normal mesenchymal tissues. Application of a histologic grading system. *Arch Pathol Lab Med.* 1983;107:328-334.
47. Hindman JC. Proton resonance shift of water in the gas and liquid states. *J Chem Phy.s* 1966;44:4582-4592.
48. Hynynen K. The role of nonlinear ultrasound propagation during hyperthermia treatments. *Med Phys.* 1991;18:1156-1163.
49. Lyons BE, Obana WG, Borcich JK, Kleinman R, Singh D, Britt RH. Chronic histological effects of ultrasonic hyperthermia on normal feline brain tissue. *Radiat Res.* 1986;106:234-251.
50. Berg AT. Are febrile seizures provoked by a rapid rise in temperature? *Am J Dis Child.* 1993;147:1101-1103.
51. el Radhi AS, Banajeh S. Effect of fever on recurrence rate of febrile convulsions. *Arch Dis Child.* 1989;64:869-870.
52. McDannold N, Zadicario E, Pilatou MC, Jolesz FA. Preclinical testing of a second-generation MRI-guided focused ultrasound system for transcranial brain tumor ablation. Presented at the 16th Scientific Meeting, International Society for Magnetic Resonance in Medicine, Toronto, Ontario, Canada, 2008.
53. Sokka SD, King R, Hynynen K. MRI-guided gas bubble enhanced ultrasound heating in in vivo rabbit thigh. *Phys Med Biol.* 2003;48:223-241.

Acknowledgments

This study was supported by NIH grant R01EB003268. InSightec funded the clinical trial. The authors extend their gratitude to Eyal Zadicario, Joanne O'Hara, Jason White, and Kevin Lanctot for their help with these treatments.

COMMENT

The authors present their initial experience in 3 patients with delivery of focused ultrasound energy transcranially to try to achieve thermocoagulation of deep-seated brain tumors noninvasively. In the first patient, 650 W were delivered in 20-second sonications; in the second 2 patients, 800 W were delivered in 20-second sonications. Heating of the cranium and scalp was mitigated with a water-cooling jacket, and targeting was achieved with proprietary targeting software and magnetic resonance imaging. Temperature magnetic resonance imaging was used for target and surrounding parenchymal temperature measurement. This study represents pilot data on the efficacy of transcranial delivery of multiple beams of ultrasound energy, analogous to stereotactic radiosurgical energy delivery. Constraints of the power of the device, as well as heating of the scalp and cranium with pain in 1 patient, indicate a likely narrow range of potential efficacy to achieve effective thermocoagulation without injury to bystander tissues. The authors outline their insights into the constraints of the system, specifically, the power limitation of the existing device and the limitation of heating of the surrounding bystander brain tissue, cranium, and scalp. However, this suggests a potential major hurdle to clinical utility—the sharpness in fall-off of the heating effect at the target versus surrounding tissue, making conformal thermocoagulation without injuring the surrounding normal tissue potentially very difficult to obtain. Improvements in device design, outlined by the authors, include increasing the power, doubling the elements in the phased array, lowering the ultrasound frequency, and boosting focal heating by bubble-enhanced absorption, may help to broaden the range between effective thermocoagulation and avoiding heating surrounding tissue.

Matthew Smyth
St. Louis, Missouri